the Transition Region Between Smooth and Rough Pipe Laws," *J. Inst. Civil Engrs.*, London, **11**, p. 133 (1939).
Darby, R., "Transient and Steady State Rheological Properties of Very Dilute Drag Reducing Polymer Solutions," *Trans. Soc. Rheol.*, **14**, p. 185 (1970).
Darby, R., "A Review and Evaluation of Drag Reduction Theories," *NRL Memo Report*, No. 2446, Naval Research Laboratory, Washington, DC (1972).
Davies, J. T., *Turbulence Phenomena*, p. 51, Academic Press, New York (1972).
Elata, C., J. Lehrer, and A. Kahanovitz, "Turbulent Shear Flow of Polymer Solutions," *Israel J. Tech.*, **4**, p. 87 (1966).
Fortuna, G., and T. J. Hanratty, "Use of Electrochemical Techniques to Study the Effect of Drag-Reducing Polymers on Flow in the Viscous Sublayer," *AIChE Symp. Ser.*, **67**, 111, p. 90 (1971).
Hanratty, T. L., and L. G. Chorn, "Turbulence Properties in the Region of Maximum Drag Reduction," *Proced. of the Fifth Biennial Symp. on Turbulence*, Univ. of Missouri-Rolla, G. K. Patterson and J. L. Zakin, Eds., 169 (1977).
Hoyt, J. W., "Drag-Reduction Effectiveness of Polymer Solutions in the Turbulent-Flow Rheometer: A Catalog," *Polymer Letters*, **9**, p. 851 (1971).
Hoyt, J. W., "The Effect of Additives on Fluid Friction," *J. Basic Eng.*, **94D**, p. 258 (1972).
Ivanyuta, Yu F., I. D. Zheltukhin, and N. A. Sergievskii, "Measurement of the Spectrum of the Longitudinal Component of the Pulsation Velocity in the Turbulent Boundary Layer of a Non-Newtonian Fluid," *Fluid Mech.-Soviet Res.*, **1**, 3, p. 82 (1972).
Lumley, J. L., "Drag Reduction in Turbulent Flow by Polymer Additives," *J. Polym. Sci. Macromol. Rev.*, **7**, p. 263 (1973).
Metzner, A. B., and A. P. Metzner, "Stress Levels in Rapid Extensional Flows of Polymeric Fluids," *Rheol. Acta*, **9**, p. 174 (1970).
Ng, K. S., and J. P. Hartnett, "Effect of Mechanical Degradation on Pressure Drop and Heat Transfer Performance of Polyacrylamide Solutions in Turbulent Pipe Flow," *Studies in Heat Transfer*, J. P. Hartnett, T. F. Irvine, Jr, E. Pfender, and E. M. Sparrow, Eds., Hemisphere Publishing Corp., p. 297 (1979).
Patterson, G. K., and J. L. Zakin, "Prediction of Drag Reduction with a Viscoelastic Model," *AIChE J.*, **14**, p. 434 (1968).
Patterson, G. K., and F. A. Seyer, "Velocity Measurements in Turbulent Flow of Viscoelastic Solutions," *Can. J. Chem. Eng.*, **50**, p. 714 (1972).
Seyer, F. A., and A. B. Metzner, "Turbulence Phenomena in Drag Reducing Systems," *AIChE J.*, **15**, p. 426 (1969).
Townsend, P., "Numerical Solutions of Some Unsteady Flows of Elasto-Viscous Liquids," *Rheol. Acta*, **12**, p. 13 (1973).
Tsai, C. F., and R. Darby "Nonlinear Viscoelastic Properties of Very Dilute Drag Reducing Polymer Solutions," *J. Rheol.*, **22**, p. 219 (1978).
Virk, P. S., "Drag Reduction Fundamentals," *AIChE J.*, **21**, p. 505 (1975).
Wang, C. B., "Correlation of the Friction Factors for Turbulent Pipe Flow of Dilute Polymer Solutions," *I&EC Fund.*, **11**, p. 546 (1972).

Manuscript received July 6, 1982; revision received May 11, and accepted May 19, 1983.

Modeling of Growth Rate Dispersion of Citric Acid Monohydrate in Continuous Crystallizers

A mathematical model for prediction of the crystal size distribution from a continuous crystallizer is presented. The kinetic data used for the model were obtained from batch contact nucleation experiments with citric acid monohydrate. In these experiments, the distribution of growth rates as well as the initial size distribution were estimated. Results from the model indicate that the excess number of crystals usually present at small sizes in continuous crystallizers is due to growth rate dispersion (where crystals of the same size may have different growth rates) and not size dependent growth.

K. A. BERGLUND and M. A. LARSON

Department of Chemical Engineering
Iowa State University
Ames, IA 50011

SCOPE

The population balance technique developed by Randolph and Larson (1971) has been used extensively for both kinetic measurement and modeling of continuous mixed suspension, mixed product removal (MSMPR) crystallizers. When the assumptions of size independent crystal growth, all crystals with equal growth (i.e., no growth rate dispersion) and all nuclei formed at a near zero size are invoked, a semilogarithmic relation is predicted between crystal population density and size. Experimental evidence from continuous crystallizers, however, has shown that at lower crystal sizes (<20 μm) orders of magnitude more crystals are present than are predicted by this relation. Clearly any or all of the assumptions may be in error.

The importance of the deviation from the model is that the semilogarithmic population density-crystal size plot is used to determine kinetic data. When the model holds and a straight line is produced, the growth rate is determined from the slope and the nucleation rate is determined from both the slope and intercept. When curvature occurs, the slope no longer has a single value and the intercept must be determined by some means of nonlinear extrapolation. In order to develop unambiguous kinetic models, it is necessary to understand the causes for the curvature.

The present study made use of data taken previously (Berglund, and Larson, 1982) in contact nucleation experiments with the citric acid monohydrate-water system. These data suggest that size independent growth rate, growth rate dispersion, and initial size distribution are present. Use was then made of probability transform techniques to develop a model for a continuous MSMPR crystallizer that accounts for these phenomena. Studies with the model concentrated on the effects of growth rate distribution, initial size distribution, and the interaction between the two distributions on the product population density.

Correspondence concerning this paper should be directed to K. A. Berglund, Department of Chemical Engineering, Michigan State University, East Lansing, MI 48824

CONCLUSIONS AND SIGNIFICANCE

From the modeling studies of continuous mixed suspension, mixed product removal (MSMPR) crystallizers operating in the contact nucleation regime, it was found that the curvature in the semilogarithmic population density crystal size plots can be explained on the basis of growth rate dispersion coupled with an initial size distribution of the nuclei. Furthermore, it was found the initial size distribution had a small effect, while the growth rate distribution had a large effect on the predicted crystal size distribution (CSD). When the two distributions were combined into a bivariate distribution which allows a linear dependence of growth rate on initial size, little change was observed.

The modeling results combined with previous experimental results on the citric acid monohydrate-water system suggest that the most important factor contributing to nonideality in the CSD from a continuous MSMPR crystallizer is growth rate dispersion. It is, therefore, concluded that this factor should be the focus in future work to control CSD.

INTRODUCTION

The population balance technique developed by Randolph and Larson (1971) predicts the steady state population density for an ideal continuous mixed suspension, mixed product removal (MSMPR) crystallizer to be

$$n(L) = n^0 \exp(-L/G\tau). \tag{1}$$

$$\text{where } n(L) = \lim_{\Delta L \to 0} \frac{\Delta N}{\Delta L}.$$

This relationship, when plotted on a semilogarithmic scale, will produce a straight line. However, in MSMPR contact nucleation studies (e.g., Sikdar and Randolph, 1976; Hartel et al., 1980) an upward curvature has been found to exist at smaller sizes ($\approx$20 μm). Various causes for this deviation have been suggested, but the three usually considered are: i) nuclei formed in a finite size range; ii) size dependent growth rate of nuclei; and iii) growth dispersion (a distribution of growth rates for crystals of a given size). Of these causes ii and iii have been modeled in the literature.

The most widely used model for size dependent growth is that proposed by Abegg et al. (1968). With this model, the expression for the steady state population density for an ideal MSMPR crystallizer becomes

$$n(L) = n^0 \exp(1/G_0\tau a(1-b))(1+aL)^{-b} \exp(-(1+aL)^{1-b}/G_0\tau a(1-b)). \tag{2}$$

This equation has been successfully fit to experimental data from real MSMPR crystallizers (e.g., Rousseau and Parks, 1981); however, physical interpretation of the constants is inconclusive. In addition, size dependent growth is the only factor included in the model.

Janse and deJong (1979) developed a model for growth dispersion in MSMPR crystallizers. This was accomplished by defining a new distribution called the modified population density defined as

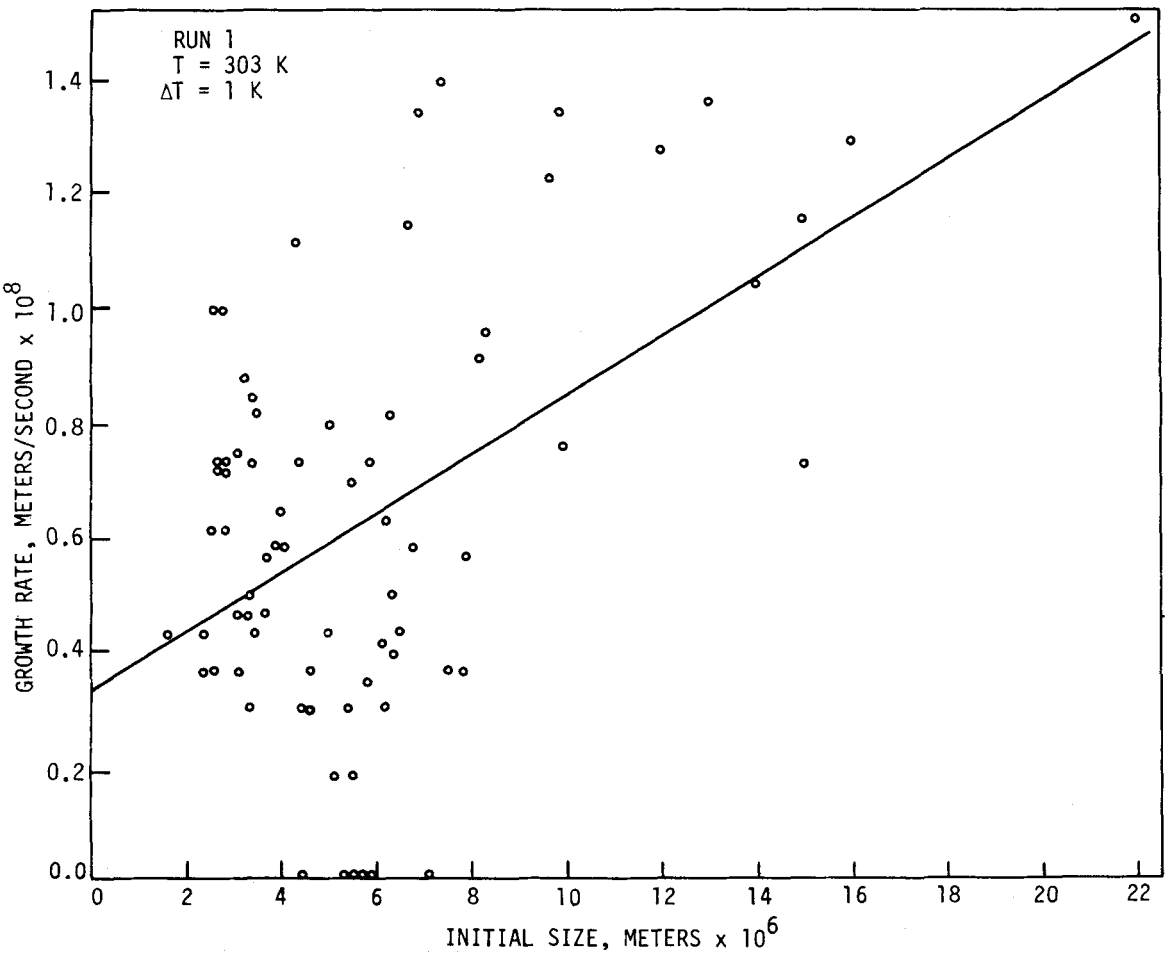

Figure 1. Growth rate vs. initial size for citric acid monohydrate at 1 K supercooling.

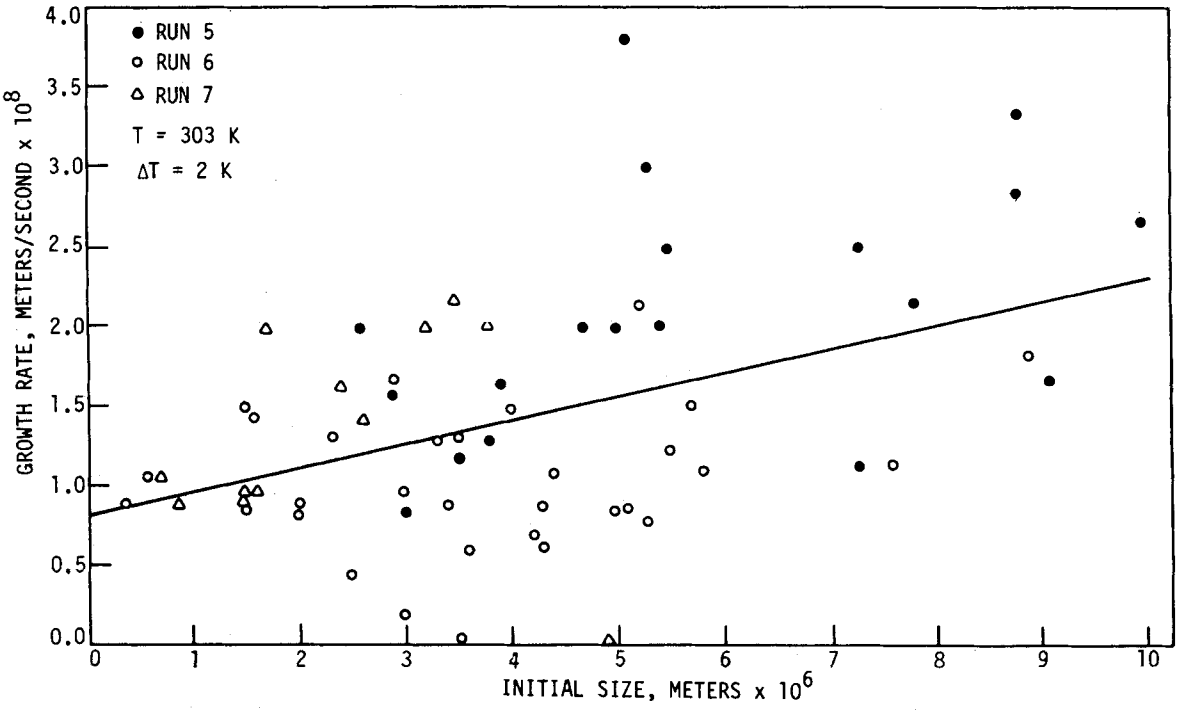

Figure 2. Growth rate vs. initial size for citric acid monohydrate at 2 K supercooling.

$$f(L,G) = \lim_{\Delta L,\Delta G \to 0} \frac{\Delta N}{\Delta L \Delta G} \tag{3}$$

where $n(L) = \int_0^\infty f(L,G)dG.$

This is simply a bivariate distribution of size and growth rate which may be used to replace $n(L)$ in the population balance. To solve the modified population balance they assumed size independent growth and that the nuclei were formed at a single size with a growth rate that was gamma distributed. When solved, the final result for population density was

$$n(L) = n^0 \left(1 + \frac{L}{q\tau}\right)^{1-r}. \tag{4}$$

This model results in the desired curvature in a semilogarithmic population density size plot.

MODEL

Recently Berglund (1981) and Berglund and Larson (1982) studied contact nucleation of citric acid monohydrate (the same system studied by Sikdar and Randolph (1976)) and found that there were distributions of both sizes and growth rates of the nuclei. The relationship between growth rate and initial size was approximated by a straight line as is shown in Figures 1, 2 and 3. This was determined by performing linear regressions using the Statistical Analysis System (SAS). The correlation of growth rate to

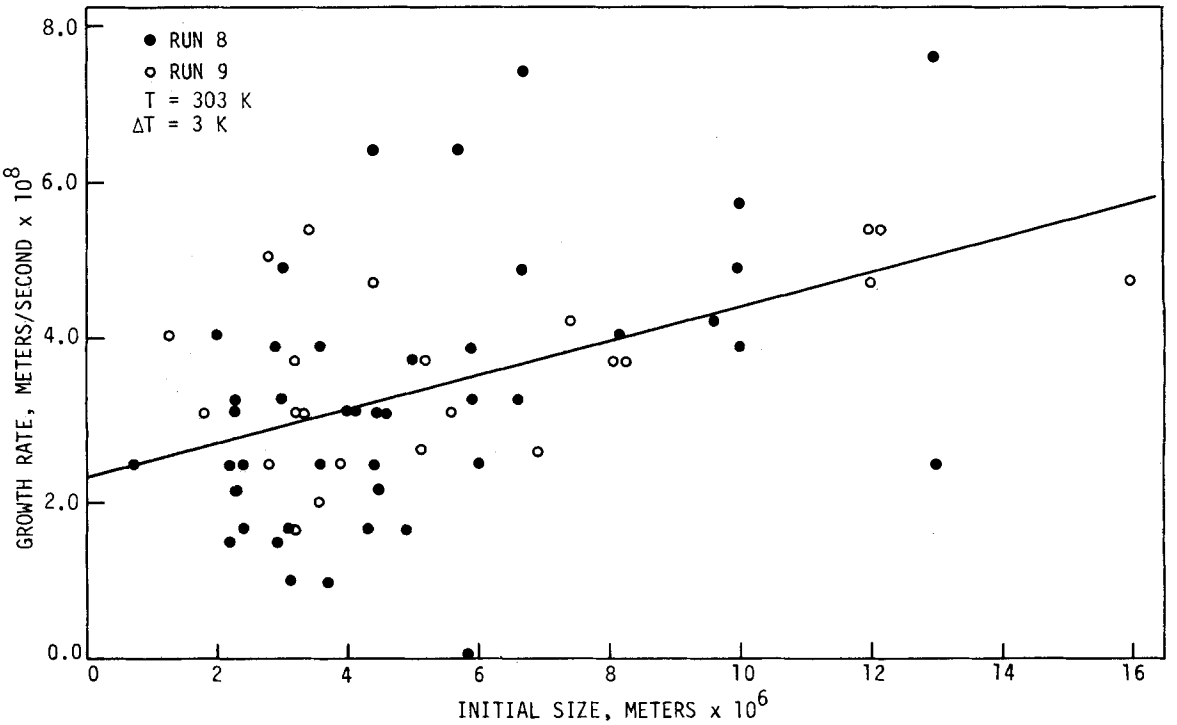

Figure 3. Growth rate vs. initial size for citric acid monohydrate at 3 K supercooling.

TABLE 1. LINEAR REGRESSIONS OF GROWTH RATE VS. INITIAL SIZE FOR THE DATA OF BERGLUND AND LARSON (1982) SHOWN IN FIGURES 1, 2 AND 3

Supercooling, ΔT, K	Slope, $s^{-1} \times 10^4$	Intercept $m/s \times 10^8$	Correlation Coefficient
1	5.2	0.33	0.5044
2	15.0	0.82	0.4583
3	22.0	2.3	0.4623

TABLE 2. CALCULATED F VALUES BASED ON TYPE I SUM OF SQUARES* FOR TERMS IN THE POLYNOMIAL FIT OF GROWTH RATE VS. INITIAL SIZE ($G = C_o + C_1L_i + C_2L_i^2 + C_3L_i^3$) FOR THE DATA OF BERGLUND AND LARSON (1982) SHOWN IN FIGURES 1, 2 AND 3

Supercooling, ΔT, K	Linear L_i	Quadratic L_i^2	Cubic L_i^3	95% F value**	99% F value**
1	26.4	1.89	6.43	3.98	7.03
2	16.7	1.99	0.40	4.00	7.07
3	17.3	0.19	1.62	3.99	7.06

* The Type I sum of squares is the sequential sum of squares resulting from the addition of subsequent terms in the model.

** Tabulated F values. If calculated F value is larger than tabulated F value, term is significant.

initial size was found significant at the 95% confidence level in spite of the wide scatter in the data as evidenced by the low correlation coefficients in Table 1. After initial size was found significant, the significance of higher order terms was assessed. This was accomplished by adding quadratic and cubic terms of initial size to the existing linear model. Table 2 lists the F-test values for the various terms of growth rate versus initial size. From these F values it was observed that only in the case of the cubic term at $\Delta T = 1$ K are any of the quadratic or cubic terms significant at the 95% level. At the 99% level none of these terms are significant. The conclusion

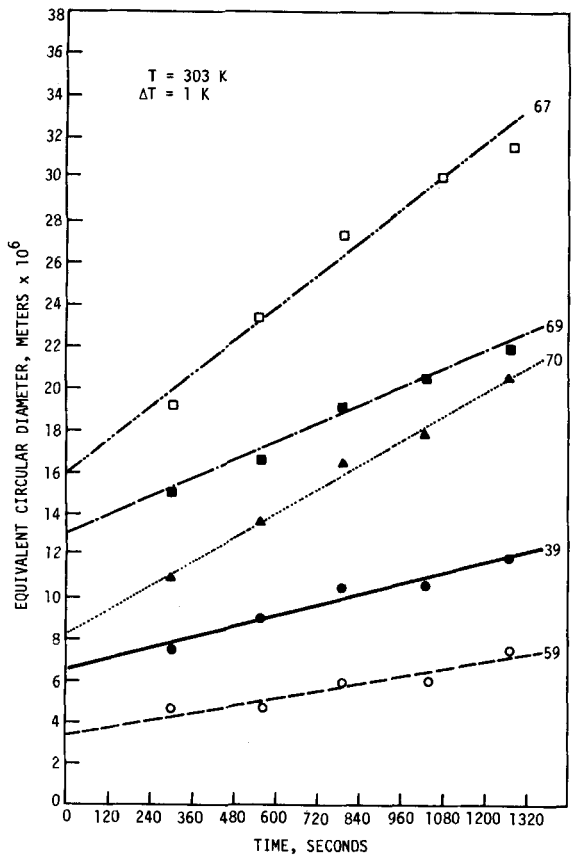

Figure 4. Size vs. time for citric acid monohydrate at 1 K supercooling. Each line is for an individual crystal.

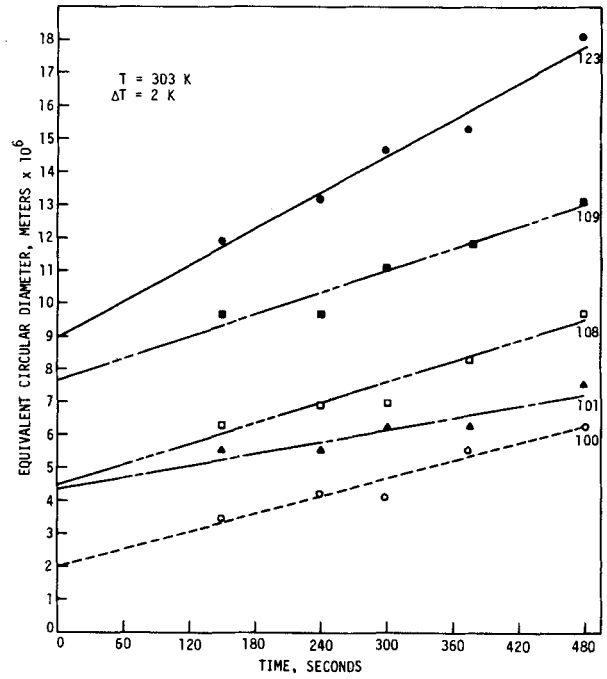

Figure 5. Size vs. time for citric acid monohydrate at 2 K supercooling. Each line is for an individual crystal.

drawn from these results is that a linear model describes the correlation of growth rate to initial size.

Plots of equivalent circular diameter (a measurement analogous to Coulter Counter data) versus time were constructed for each nuclei observed. The slope of such a plot is the crystal growth rate and the intercept is the initial size. The plots shown in Figures 4, 5 and 6 demonstrate linearity which corresponds to a constant growth rate, i.e., size independent growth. In addition, the plots have different slopes and intercepts corresponding to growth rate and initial size distributions, respectively. In view of these results

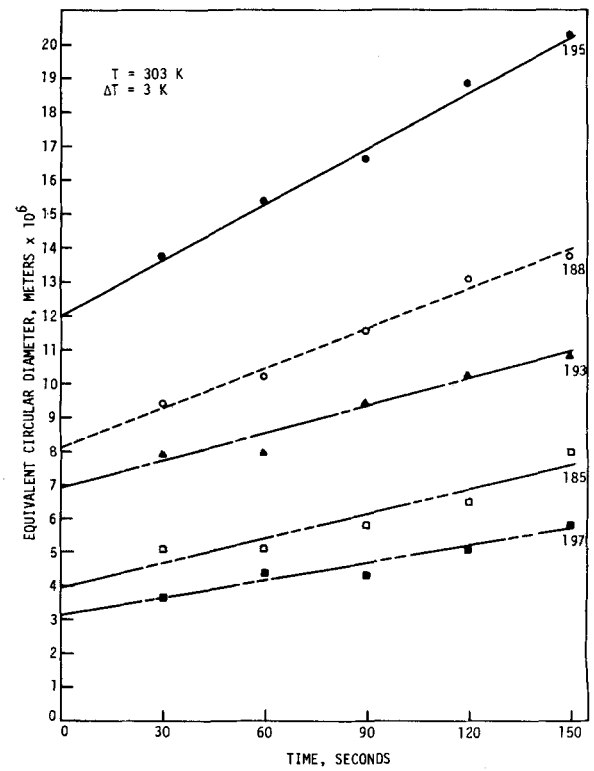

Figure 6. Size vs. time for citric acid monohydrate at 3 K supercooling. Each line is for an individual crystal.

TABLE 3. PARAMETERS OF THE GAMMA DISTRIBUTIONS (EQS. 9 AND 10) CALCULATED USING THE METHOD OF MOMENTS FROM THE DATA OF BERGLUND AND LARSON (1982) SHOWN IN FIGURES 1, 2 AND 3

ΔT, K	Initial Size λ_1, m × 10^6	λ_2	Correlation Coefficient	Growth Rate γ_1, m/s × 10^8	γ_2	Correlation Coefficient
1	2.3	2.6	0.9766	0.22	2.9	0.9767
2	1.4	3.0	0.9890	0.40	3.5	0.9921
3	2.0	2.6	0.9896	0.68	5.1	0.9916

a different model is necessary to describe the physical situation.

The size of any crystal in the product stream of a crystallizer may be described by multiplying the residence time by its individual growth rate and adding its initial size, thus

$$L = L_i + Gt. \tag{5}$$

Since L_i, G and t all have distributions, their population density functions (*pdf*) are designated $\lambda(L_i)$, $\gamma(G)$, and $\theta(t)$, respectively. Furthermore, Eq. 5 is the description of a random variable L, so solution of the distribution of the random variable L yields the population size density of the product stream.

As a first approximation to the solution it is assumed there is no dependence of G on L_i. This corresponds to zero slopes in Figures 1, 2 and 3. This assumption will be studied in subsequent calculations.

To compute the *pdf* for L it is necessary to first compute the *pdf* for Gt. This is accomplished through use of the Mellin transform and convolution (from Griffin, 1975) for products of random variables. Setting $x = Gt$, the result is

$$f(x) = \int_0^\infty \frac{1}{t}\,\gamma\left(\frac{x}{t}\right)\theta(t)dt. \tag{6}$$

Using this result for x, the pdf for the random variable $L_i + x$ (or $L_i + Gt$) is determined using the Laplace transform and convolution for sums of random variables. The final result is

$$n(L) = \int_0^L \int_0^\infty \lambda(s)\,\frac{1}{t}\,\gamma\left(\frac{L-s}{t}\right)\theta(t)dtds. \tag{7}$$

This result is general for $n(L)$ regardless of the forms of λ, γ, or θ.

Since the object of the present study is an MSMPR crystallizer, the residence time distribution is (from Levenspiel, 1972)

$$\theta(t) = \frac{1}{\theta'}\exp(-t/\theta') \tag{8}$$

where θ' is the mean residence time used in MSMPR analyses.

The distributions for $\gamma(G)$ and $\lambda(L_i)$ correspond to the marginal distributions of the bivariate distribution of Figures 1, 2 and 3. In other words, these distributions can be found by determining the distribution of initial size in Figures 1, 2 and 3 ignoring the growth rate and *vice versa* for the growth rate distribution. When this is done for all sets of data, the two distributions are found to be gamma distributions which have the form

$$\gamma(G) = \frac{1}{\gamma_1^{\gamma_2}\Gamma(\gamma_2)}\,G^{\gamma_2-1}\exp(^{-G}/_{\gamma_1}) \tag{9}$$

$$\text{and } \lambda(L_i) = \frac{1}{\lambda_1^{\lambda_2}\Gamma(\lambda_2)}\,L_i^{\lambda_2-1}\exp(^{-L_i}/_{\lambda_1}). \tag{10}$$

The parameters γ_1, γ_2, λ_1, and λ_2 are determined by using the method of moments, and the correlation coefficients are found by testing the fit with the Statistical Analysis System (SAS). The parameter values determined for the data in Figures 1, 2 and 3 are shown in Table 3. The final expression for $n(L)$ takes the form

$$n(L) = \int_0^L \int_0^\infty \left[\frac{1}{\lambda_1^{\lambda_2}\Gamma(\lambda_2)}\,s^{\lambda_2-1}\exp\left(\frac{-s}{\lambda_1}\right)\right]\left[\frac{1}{t}\right] \times \left[\frac{1}{\gamma_1^{\gamma_2}\Gamma(\gamma_2)}\left(\frac{L-s}{t}\right)^{\gamma_2-1}\exp\left(-\frac{(L-s)}{\gamma_1 t}\right)\right] \times \left[\frac{1}{\theta'}\exp(-t/\theta')\right]dtds \tag{11}$$

Due to the complex nature of this expression an analytical solution is not possible.

Equation 11 is based upon the assumption that growth rate does not depend on initial size. To relax this assumption, the population density of size is considered to be described by some manipulation of the distribution $f_1(L_i,G)f_2(t)$. The first term includes the dependence of growth rate on initial size, while the second is the same residence time distribution as before. The transformation procedure from Peebles (1980) results in a distribution for L. The variables of interest are designated in the following way

$$y_1 = G \tag{12a}$$

$$y_2 = L_i \tag{12b}$$

$$y_3 = L_i + Gt = L \tag{12c}$$

In general it can be written

$$g(y_1,y_2,y_3) = f\left(y_1,y_2,\frac{y_3-y_1}{y_2}\right)/J/ \tag{13}$$

So for the present case the following expression can be written

$$f_1(L_i,G)f_2(t) = f_1(L_i,G)f_2\left(\frac{L-L_i}{G}\right)/J/ \tag{14}$$

where the Jacobian's determinant equals $1/G$. The general expression for $n(L)$ is thus

$$n(L) = \int_0^\infty \int_0^\infty f_1(L_i,G)f_2\left(\frac{L-L_i}{G}\right)\frac{1}{G}\,dL_i dG \tag{15}$$

The procedure used to find Eq. 15 is found in most texts on mathematical statistics and is merely outlined here. The remaining task here is to determine an expression for f_1; f_2 is the same as used before. Ghirtis (1967) presented a bivariate gamma distribution which requires the marginal distributions to be gamma distributions and the regression of the two variables to be linear. These two conditions are met by the data of Figures 1, 2 and 3, and the distribution is given by

$$f_1(L_i,G) = \frac{\exp\left(\frac{-L_i}{\lambda_3}-\frac{G}{\lambda_3}\right)}{\lambda_3^{\lambda_4}\gamma_3^{\gamma_4}\Gamma(\xi)\Gamma(\lambda_4)\Gamma(\gamma_4)}\int_0^{u'} u^{\xi-1}(L_i-\lambda_3 u)^{\lambda_4-1} \cdot (G-\gamma_3 u)^{\gamma_4-1}e^u du \tag{16}$$

where u' is the minimum of G/γ_3 and L_i/λ_3. Once again the distribution parameters are determined by the method of moments. The values determined for the data in Figures 1, 2 and 3 are shown in Table 4. The final expression for $n(L)$ is

TABLE 4. PARAMETERS FOR THE BIVARIATE GAMMA DISTRIBUTION (EQ. 16) CALCULATED USING THE METHOD OF MOMENTS FROM THE DATA OF BERGLUND AND LARSON (1982) SHOWN IN FIGURES 1, 2 AND 3

ΔT, K	λ_3, m × 10^6	γ_3, m/s × 10^8	ξ	λ_4	γ_4
1	2.3	0.22	1.3	1.2	1.6
2	1.4	0.40	1.5	1.5	2.1
3	2.0	0.68	1.7	0.95	3.5

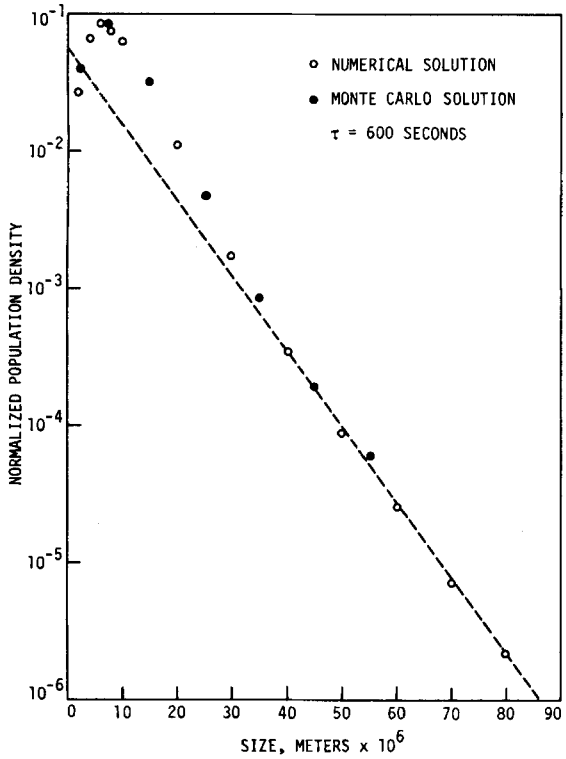

Figure 7. Comparison of numerical solution of Eq. 11 to Monte Carlo simulation for the case where growth rate is independent of initial size at 1 K supercooling. Parameters for the gamma distribution are from Table 3.

$$n(L) = \int_0^\infty \int_0^\infty \frac{\exp\left(\frac{-L_i}{3} - \frac{G}{3}\right)}{\lambda_3^{\lambda_4}\gamma_3^{\gamma_4}\Gamma(\xi)\Gamma(\lambda_4)\Gamma(\gamma_4)} \times \int_0^{u'} u^{\xi-1}(L_i - \lambda_3 u)^{\lambda_4-1}(G - \gamma_3 u)^{\gamma_4-1} e^u du \cdot \left[\frac{1}{\theta'}\exp\left(\frac{-(L-L_i)}{G\theta'}\right)\right]\left[\frac{1}{G}\right] dL_i dG. \quad (17)$$

RESULTS AND DISCUSSION

Equation 11, which assumes independence between initial size and growth rate, was solved using a Simpson's approximation and also a Monte Carlo simulation. A mean residence time of 600 seconds was used in the simulation since it is on the same order as that used by Sikdar and Randolph (1976). Normalized population density versus size plots are presented in Figures 7, 8 and 9 for 1, 2 and 3 K undercooling, respectively. Common among all of the plots is an upward curvature at lower sizes and a linear region at larger sizes. Also, all plots have a sharp downward curvature as zero size is approached. This downward curvature at low sizes is attributed to the distribution used to approximate the initial size distribution. Since a gamma distribution (which passes through the origin) was used, the resulting product CSD calculated from the model must also pass through the origin. The experimental technique used for measurement of the initial size distribution was not sensitive enough to thoroughly establish the distribution below about 2×10^{-6}m. This resulted in the approximation which leads to the downward curvature.

A more interesting feature of Figures 7, 8 and 9 is the growth rate calculated from the linear region. Assuming that this region can be described by Eq. 1, the growth rates can be obtained from the slopes. Table 5 compares the growth rate calculated from Eq. 1 with the mean growth rate calculated from the experimentally determined growth rate distribution. This indicates in all cases that the growth rate calculated from the slope is larger than the actual

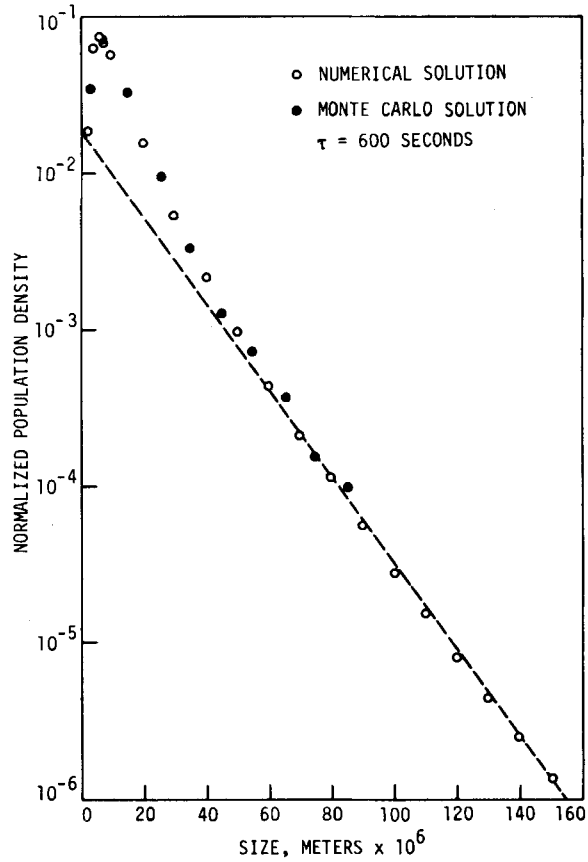

Figure 8. Comparison of numerical solution of Eq. 11 to Monte Carlo simulation for the case where growth rate is independent of initial size at 2 K supercooling. Parameters for the gamma distribution are from Table 3.

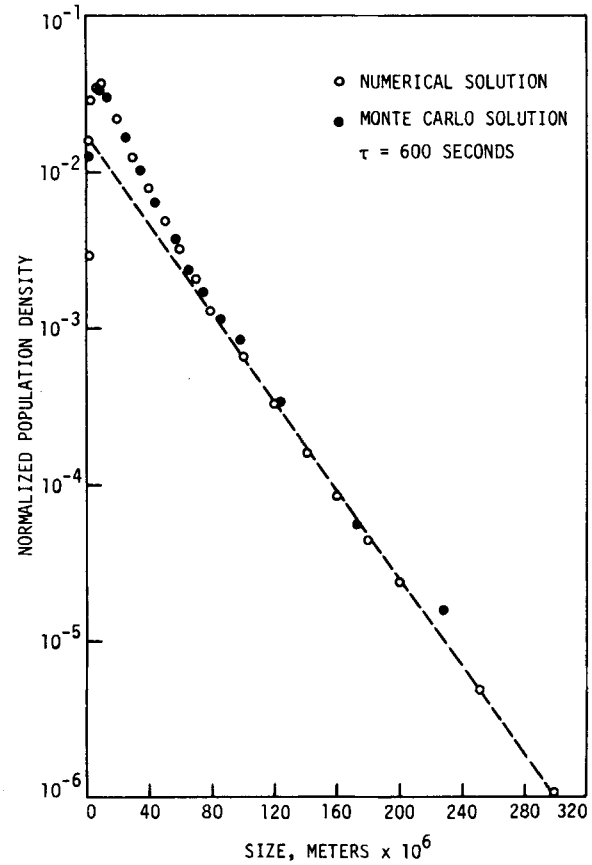

Figure 9. Comparison of numerical solution of Eq. 11 to Monte Carlo simulation for the case where growth rate is independent of initial size at 3 K supercooling. Parameters for the gamma distribution are from Table 3.

TABLE 5. COMPARISON OF GROWTH RATE FROM LINEAR REGION OF SEMILOGARITHMIC POPULATION DENSITY-SIZE PLOT* WITH ACTUAL MEAN GROWTH RATE**

ΔT, K	Actual Mean,** m/s × 10^8	From Linear Region,* m/s × 10^8
1	0.63	1.3
2	1.4	2.7
3	3.5	5.2

* Determined from the linear portion of the plots in Figures 7, 8 and 9.
** Calculated from the growth rate distribution parameters in Table 3.

growth rate. The reason for this behavior is the slow growth rates of some crystals. These slow growing crystals do not become viable nuclei to seed the distribution at larger sizes since they are washed out of the crystallizer before they can grow to a large size. Furthermore, this demonstrates how the phenomenon of growth dispersion can be misinterpreted as size dependent growth. In other words, an MSMPR crystallizer can be thought of as a crystallizer which classifies crystals on the basis of their growth rates. Crystals don't grow faster because they are larger, rather they become larger because they grow faster.

In a subsequent set of calculations the effects of the width of the growth rate distribution and initial size distribution were studied. When the initial size distribution is widened while holding the mean size and the entire growth rate distribution constant, no discernible effect is observed on the final distribution. However, by varying the width of the growth rate distribution while holding the mean growth rate and initial size distribution constant, drastic changes can be obtained. Figure 10 shows the effect of the coefficient of variation (C.V.), which is the standard deviation of the growth rate distribution divided by the mean, of the growth rate distribution on the final distribution. It can easily be seen that as the C.V. is increased the curvature increases. This would correspond to larger growth rates being calculated from the slope as the C.V. increases.

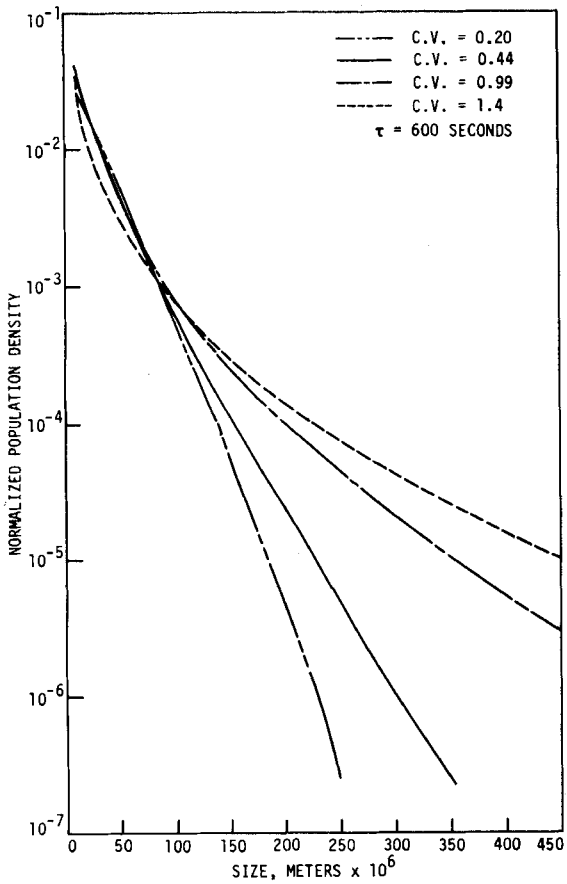

Figure 10. Effect of growth rate coefficient of variation (C.V.) for 3 K supercooling using numerical solution of Eq. 11. Parameters from Table 3 were used for λ_1, λ_2, and γ_1. γ_2 was varied since C.V. = $1/\sqrt{\gamma_2}$.

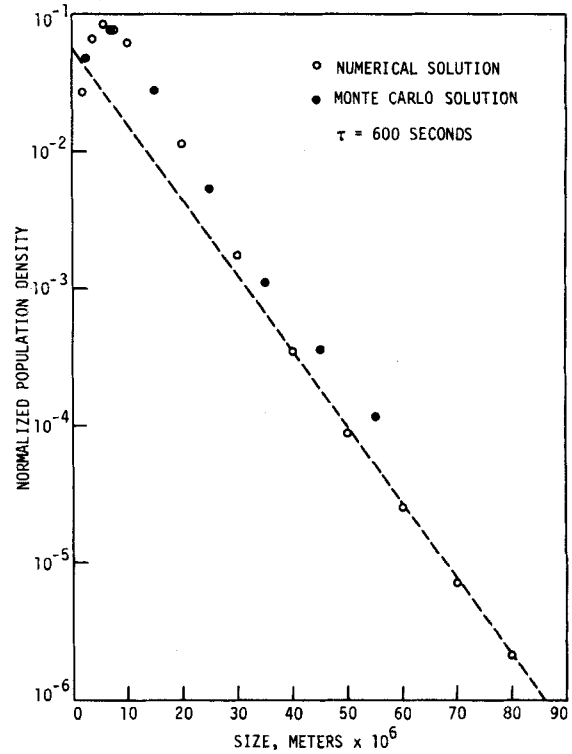

Figure 11. Comparison of numerical solution of independent case (Eq. 11 with parameters from Table 3) with Monte Carlo simulation of dependent case (Eq. 17 with parameters from Table 4) at 1 K supercooling.

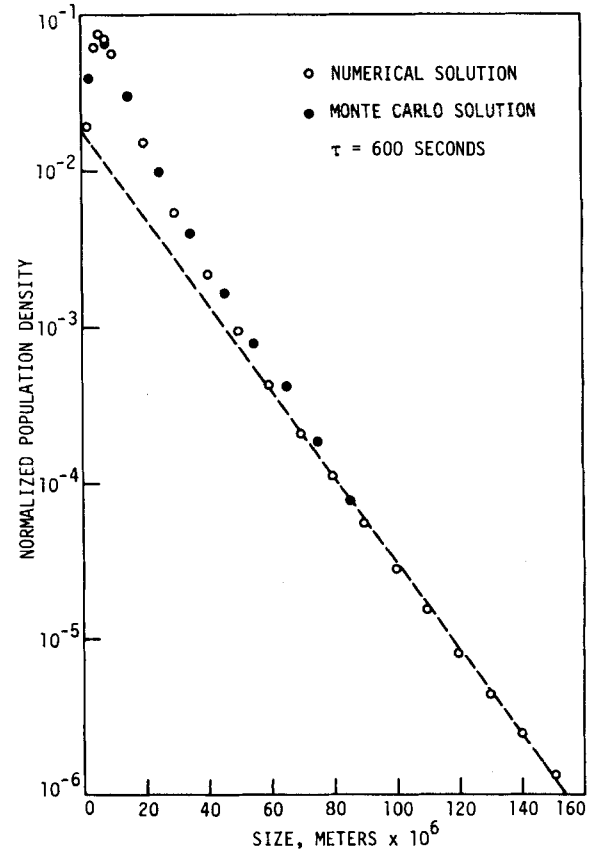

Figure 12. Comparison of numerical solution of independent case (Eq. 11 with parameters from Table 3) with Monte Carlo simulation of dependent case (Eq. 17 with parameters from Table 4) at 2 K supercooling.

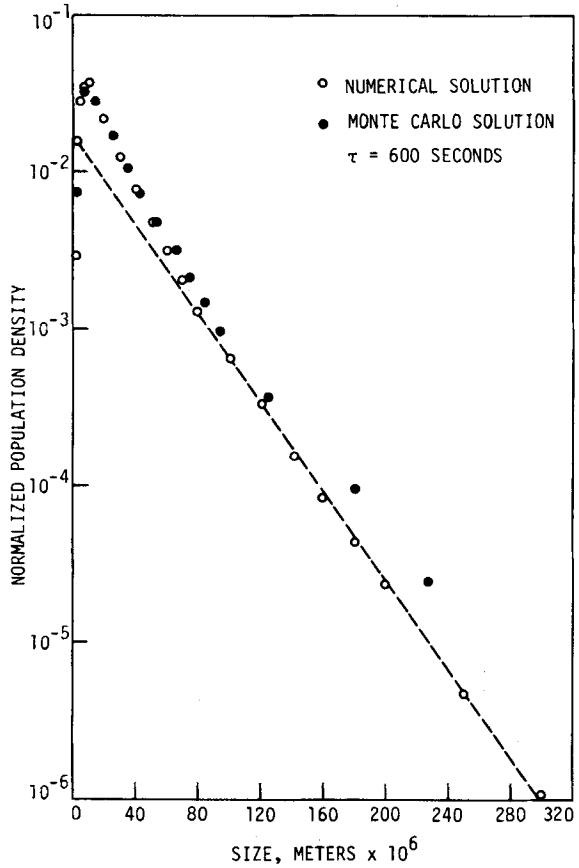

Figure 13. Comparison of numerical solution of independent case (Eq. 11 with parameters from Table 3) with Monte Carlo simulation of dependent case (Eq. 17 with parameters from Table 4) at 3 K supercooling.

To relax the assumption of independence of initial size and growth rate, a Monte Carlo simulation of Eq. 17 was performed. Figures 11, 12 and 13 compare this Monte Carlo solution to the numerical solution for independence. From these results it can be seen that the dependent case has a tendency to curve more at larger sizes. In general, however, fairly good agreement is obtained between the two cases, and it would appear that inclusion of dependence adds a great deal of complexity while adding little information.

The model presented has large implications with respect to the interpretation of MSMPR experiments. The occurrence of curvature in the semi-logarithmic population density-size plot does not simply imply size dependent growth rates as often as has been assumed. It is clear that new means of interpreting these results must be developed. In addition, it is also evident that MSMPR crystallizer experiments alone should not be used to determine mechanisms. The photomicroscopic technique used to collect data for the present work is a possible complementary experiment to be used with MSMPR experiments. This will avoid erroneous models to be assumed in analyzing data.

CONCLUSIONS

1. A model has been presented that demonstrates marked curvature of a semilogarithmic population density vs. size plot for an MSMPR crystallizer in the absence of size dependent growth.
2. Apparent size dependent growth is probably due to slow growing crystals being washed out.
3. The distribution of growth rates has a large effect upon the product CSD, while the initial size distribution has a smaller effect.
4. Inclusion of growth rate dependence upon initial size does not alter results a great deal.

ACKNOWLEDGMENTS

The authors wish to thank H. T. David and S. K. Fahrenholtz, Department of Statistics, Iowa State University, for consultations leading to the completion of this work. The support of Amoco Oil Co. and NSF under the grant number ENG77-06054 is acknowledged.

LITERATURE CITED

Abegg, C. F., J. D. Stevens, and M. A. Larson, "Crystal Size Distributions in Continuous Crystallizers when Growth Rate is Size Dependent," *AIChE J.*, **14**(1), p. 118 (1968).
Berglund, K. A., "Formation and Growth of Contact Nuclei," Ph.D. Dissertation, Iowa State University of Science and Technology, Ames (1981).
Berglund, K. A., and M. A. Larson, "Growth of Contact Nuclei of Citric Acid Monohydrate," *AIChE Sym. Ser.*, **78**(215), p. 9 (1982).
Ghirtis, G. C., "Some Problems of Statistical Inference Relating to the Double-Gamma Distribution," *Trabajos de Estadistica*, **18**, p. 67 (1967).
Giffin, W. C., *Transform Techniques for Probability Modeling*, Academic Press, New York (1975).
Hartel, R. W., K. A. Berglund, S. M. Gwynn, P. M. Schierholz, and V. G. Murphy, "Crystallization Kinetics for the Sucrose-Water System," *AIChE Sym. Ser.*, **76**(193), p. 65 (1980).
Janse, A. H., and E. J. deJong, "Growth and Growth Dispersion," *Industrial Crystallization 78*, E. J. deJong and A. H. Janse, Eds., North Holland Publishing Co., Amsterdam (1979).
Levenspiel, O., *Chemical Reaction Engineering*, John Wiley and Sons, Inc., New York (1972).
Peebles, P. Z., *Probability, Random Variables, and Random Signal Principles*, McGraw-Hill, New York (1980).
Randolph, A. D., and M. A. Larson, *Theory of Particulate Processes*, Academic Press, New York (1971).
Rousseau, R. W., and R. M. Parks, "Size Dependent Growth of Magnesium Sulfate Heptahydrate," *IEC Fund.*, **20**(1), p. 71 (1981).
Sikdar, S. K., and A. D. Randolph, "Secondary Nucleation of Two Fast Growth Systems in a Mixed Suspension Crystallizer: Magnesium Sulfate and Citric Acid Water Systems," *AIChE J.*, **22**(1), p. 110 (1976).

NOTATION

a = constant, Eq. 2
b = constant, Eq. 2
g = arbitrary population density function
G = crystal growth rate
G_0 = growth rate of zero-sized crystal
L = characteristic size of a crystal
L_i = initial characteristic size of a crystal
n = size population density function
n^0 = population density at zero size
N = number of crystals at a given size
q = constant, Eq. 4
r = constant, Eq. 4
s = dummy variable of integration, Eq. 7
t = residence time
y_1 = random variable defined by Eq. 12a
y_2 = random variable defined by Eq. 12b
y_3 = random variable defined by Eq. 12c
u = dummy variable of integration, Eq. 16
u' = minimum value of G/γ_3 and L_i/λ_3
γ = growth rate population density function
γ_1 = scale parameter for Eq. 9
γ_2 = shape parameter for Eq. 9
γ_3 = scale parameter for growth rate in Eq. 16
γ_4 = shape parameter for growth rate in Eq. 16
θ = residence time distribution function
θ' = mean residence time
λ = initial size population density function
λ_1 = scale parameter for Eq. 10
λ_2 = shape parameter for Eq. 10
λ_3 = scale parameter for initial size in Eq. 16
λ_4 = shape parameter for initial size in Eq. 16
ξ = parameter for dependence, Eq. 16
τ = mean residence time